Light with a twist : ray aspects in singular wave and quantum optics

Habraken, S.J.M.

2

Twisted cavity modes

2.1 Introduction

A typical optical cavity consists of two spherical mirrors facing each other. The modes of such a cavity are transverse field distributions that are reproduced after each round trip, bouncing back and forth between the mirrors [12]. The usual approach to the problem of finding the modes of an optical cavity is by considering the free propagation of light from one mirror to the other (in integral or differential form) and imposing the proper boundary conditions. In the paraxial limit the propagation through free space can be described by the paraxial wave equation, which has the Huygens-Fresnel integral equation as its integral form. The boundary condition is that the electric field vanishes at the surface of the mirrors, which implies that the mirror surfaces match a nodal plane of the standing wave that is formed by a bouncing traveling wave. Conversely, a Gaussian paraxial beam, which has spherical wave fronts, can be trapped between two spherical mirrors that coincide with a wave front, as indicated in figure 2.1. This imposes a condition on the curvatures and the spacing L of the mirrors. When the radii of curvature are R_1 and R_2, the condition is simply [12]

$$0 \leq g_1 g_2 \leq 1 \; , \tag{2.1}$$

where the parameters $g_1$and g_2 are defined by

$$g_i = 1 - \frac{L}{R_i} \tag{2.2}$$

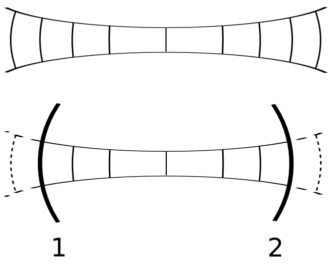

Figure 2.1: A freely propagating Gaussian beam can be trapped by mirrors that coincide with its wave fronts. Its wave fronts are then turned into nodal planes of the standing-wave pattern inside the cavity.

for $i = 1, 2$. This is precisely the stability condition of the cavity. A stable cavity is a periodic focusing system for which the round-trip magnification is equal to 1 so that it supports stable ray patterns. Such a cavity has a complete set of Hermite-Gaussian modes, with a simple Gaussian fundamental mode. For a two-mirror cavity with radii of curvature R_i and a spacing L obeying the stability condition (2.1), the modes are characterized by the Rayleigh range z_R and the round-trip Gouy phase χ that are given by [12]

$$\frac{z_\mathrm{R}^2}{L^2} = \frac{g_1 g_2 (1 - g_1 g_2)}{(g_1 + g_2 - 2g_1 g_2)^2} \qquad \text{and} \qquad \cos\left(\frac{\chi}{2}\right) = \pm\sqrt{g_1 g_2}\ . \tag{2.3}$$

The plus sign is taken if both g_1 and g_2 are positive whereas the minus sign is taken when both are negative. The wave numbers of the Hermite-Gaussian modes HG_{nm} with transverse mode numbers n and m are determined by the requirement that the phase of the field changes over a round trip by a multiple of 2π. This gives the resonance condition

$$2kL - (n + m + 1)\chi = 2\pi q \tag{2.4}$$

for the wave number k, with a longitudinal mode index $q \in \mathbb{Z}$.

It is a simple matter to generalize this method to the case of astigmatic mirrors, provided that the mirror axes are parallel. Each mirror i can be described by two radii of curvature $R_{i\xi}$ and $R_{i\eta}$, corresponding to the curvatures along the two axes. In this case of simple, or orthogonal, astigmatism the paraxial field distribution separates into a product of two contributions, corresponding to the two transverse dimensions. Stability requires that each of the two dimensions obey the stability condition (2.1) for the parameters $g_{i\xi}$ and $g_{i\eta}$, and each dimension has its own Rayleigh range and Gouy phase. The resonance condition for a cavity with simple astigmatism takes the modified form

$$2kL - \left(n + \frac{1}{2}\right)\chi_\xi - \left(m + \frac{1}{2}\right)\chi_\eta = 2\pi q\ , \tag{2.5}$$

where χ_ξ and χ_η are the Gouy phases for the ξ and η direction respectively.

The situation is considerably more complex when the axes of the two astigmatic mirrors are non-aligned. In this case of twisted cavity, the light bouncing back and forth between the mirrors becomes twisted as well and the cavity modes display general, or non-orthogonal, astigmatism, which is characterized by the absence of transverse symmetry directions. Also in this case the stability condition and the structure of the cavity modes is, in principle, determined by the requirement that the mirror surfaces match a wave front of a traveling beam. It is, however, not simple to derive the mode structure and the resonance frequencies of the cavity from this condition. The stability of a twisted cavity or lens guide as well as the propagation of the Gaussian fundamental mode, which is characterized by its elliptical intensity distribution and its elliptical or hyperbolic wave fronts, has been studied by several authors using analytical techniques [18, 34, 35, 36, 37]. Also higher-order modes have received some attention [38].

A few years ago, a general description has been given of freely propagating paraxial modes of arbitrary order with general astigmatism [17]. The method is based on the use of bosonic ladder operators in the spirit of the quantum-mechanical description of the harmonic oscillator [33] and has a simple algebraic structure. Here, we generalize this approach to study the modes to all orders of geometrically stable twisted cavities. In this case, the basis set of modes is fixed by the geometric properties of the cavity, i.e., the radii of curvature that characterize the astigmatic mirrors, their (relative) orientation and their separation. Rather than using the condition that the wave fronts match the mirror surfaces, our method is entirely based on the eigenvalues and eigenvectors of the four-dimensional ray matrix that describes the transformation of a ray after one round trip through the cavity. This matrix generalizes the $ABCD$ matrix, which describes the propagation of a ray through an isotropic optical set-up [12]. We discuss the relevant (group-theoretical) properties of this ray matrix in section 2.2. After a brief discussion of paraxial wave optics in an astigmatic cavity in section 2.3, we give in section 2.4 an operator description of fundamental Gaussian modes and higher-order modes. Here we demonstrate that the cavity modes can be directly expressed in terms of the properties of the ray matrix. In section 2.5, we discuss some physical properties of the modes including the orbital angular momentum that is due to their twisted nature and their vorticity. Explicit results for a specific case are briefly discussed in section 2.6.

2.2 Paraxial ray optics

2.2.1 One transverse dimension

In geometric optics, a light beam in vacuum is assumed to consist of a pencil of rays [29]. In each transverse plane a ray is characterized by its transverse position x and its propagation direction $\vartheta = \partial x / \partial z$, where z is the longitudinal coordinate. The angle ϑ gives the propagation direction of the ray with respect to the optical axis of the set-up through which it propagates. Both the transverse position x and the propagation direction ϑ of a ray transform under free propagation and optical elements. In lowest order of the paraxial approximation ($\vartheta << 1$)

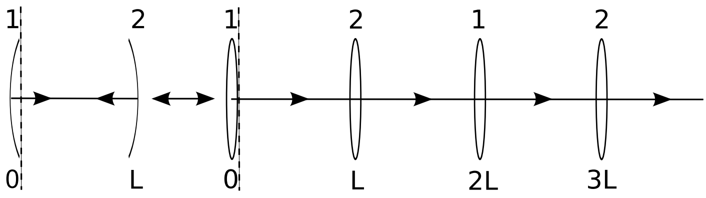

Figure 2.2: Unfolding a two-mirror cavity into an equivalent periodic lens guide; the mirrors are replaced by lenses with the same focal lengths and the reference plane is indicated by the dashed line.

this transformation is linear and can be represented by a 2×2 ray matrix acting on a ray vector $\mathfrak{r} = (x, \vartheta)^{\mathrm{T}}$

$$\begin{pmatrix} x_{\mathrm{out}} \\ \vartheta_{\mathrm{out}} \end{pmatrix} = M \begin{pmatrix} x_{\mathrm{in}} \\ \vartheta_{\mathrm{in}} \end{pmatrix} . \tag{2.6}$$

Here M is a ray matrix that transforms the input beam of the optical system into the output beam. The matrices that represent various optical elements can be found in any textbook on optics, see, for instance, reference [12]. The ray matrix for propagation through free space over a distance z is given by

$$M_{\mathrm{f}}(z) = \begin{pmatrix} 1 & z \\ 0 & 1 \end{pmatrix} . \tag{2.7}$$

The trajectory that corresponds to this transformation is a straight line with the direction angle ϑ, where the transverse position $x' = x + \vartheta z$ changes linearly with the distance z. The transformation of a ray through a paraxial thin lens can be expressed as

$$M_{\mathrm{l}}(f) = \begin{pmatrix} 1 & 0 \\ -1/f & 1 \end{pmatrix} , \tag{2.8}$$

where f is the focal length of the lens which is taken positive for a converging lens. The transverse position is invariant under this transformation. The angle ϑ, which specifies the propagation direction, changes abruptly at the location of the lens. It can be easily shown that this transformation reproduces the thin-lens equation.

The transformation matrix of a sequence of first-order optical elements can be constructed by multiplying the matrices that correspond to the various elements in the correct order. Closed optical systems such as a cavity can be unfolded into an equivalent periodic lens guide, as indicated in figure 2.2. The mirrors are replaced by thin lenses with the same focal lengths. One period of the lens guide is equivalent to a single round trip through the cavity. When we choose the transverse reference plane just right of mirror 1 (or lens 1), we can construct the ray matrix that describes the transformation of a single round trip in the form

$$M_{\mathrm{rt}} = M_{\mathrm{l}}(f_1) M_{\mathrm{f}}(L) M_{\mathrm{l}}(f_2) M_{\mathrm{f}}(L) . \tag{2.9}$$

Here L is the distance between the two mirrors of the cavity, and $f_{1,2}$ are the focal lengths of the mirrors that are related to the radii of curvature by $f_{1,2} = R_{1,2}/2$.

The ray matrices that correspond to lossless optical elements are real and have a unit determinant. Since the product of real matrices yields a real matrix whose determinant is equal to the product of the determinants, it follows that this is also true for the ray matrix that describes the transformation of any composite lossless system. In case of one transverse dimension these are the defining properties of a physical ray matrix so that the reverse of the above statement is also true: any real 2×2 matrix that has a unit determinant corresponds to the transformation of a lossless optical set-up that can be constructed from first-order optical elements. Mathematically speaking, physical ray matrices constitute the group $SL(2, \mathbb{R})$ under matrix multiplication.

An important characteristic of an optical cavity is whether it is geometrically stable or not. In many cases a cavity will support only rapidly diverging or converging ray paths. Only in specific cases does a cavity support a stable ray pattern. Usually the stability criterion of an optical cavity is formulated in terms of the parameters that characterize the geometry, i.e., the radii $R_{1,2}$ of curvature of the mirrors and the distance L between them. For our purposes, however, it is more convenient to relate the stability of a cavity to the eigenvalues λ_1 and λ_2 of the round-trip ray matrix M_{rt}. Since $\det M_{\mathrm{rt}} = 1$, it follows that $\lambda_1 \lambda_2 = 1$. If we assume that these eigenvalues are non-degenerate, i.e., $\lambda_1 \neq \lambda_2$, the corresponding eigenvectors μ_1 and μ_2 are linearly independent, so that an arbitrary input ray $\mathfrak{r}_0$ can be written as

$$\mathfrak{r}_0 = a_1 \mu_1 + a_2 \mu_2 \ . \tag{2.10}$$

After n round trips through the cavity this ray transforms to

$$\mathfrak{r}_n = M_{\mathrm{rt}}^n \mathfrak{r}_0 = a_1 \lambda_1^n \mu_1 + a_2 \lambda_2^n \mu_2 \ . \tag{2.11}$$

From this transformation of a ray through the cavity it is clear that the absolute values of the eigenvalues determine the magnification of the ray. It follows that a cavity is stable only if the absolute value of both eigenvalues is equal to 1. In case of a non-degenerate round-trip ray matrix M_{rt} this condition requires that the eigenvalues, and therefore the eigenvectors, are complex. Since M_{rt} is a real matrix, its eigenvectors as well as its eigenvalues must be each other's complex conjugates, so that

$$\mu_1 = \mu_2^* = \mu \qquad \text{and} \qquad \lambda_1 = \lambda_2^* = e^{i\chi} = \lambda \ . \tag{2.12}$$

The phase χ is the round-trip Gouy phase of the cavity, which determines its spectrum according to equation (2.4). For a real incident ray $\mathfrak{r}_0$, equation (2.10) takes the form

$$\mathfrak{r}_0 = 2\mathrm{Re}\,(a\mu) \ , \tag{2.13}$$

where $a = a_1 = a_2^*$. With equation (2.11) this leads to the expression

$$\mathfrak{r}_n = 2\mathrm{Re}\left(a\mu e^{in\chi}\right) \ , \tag{2.14}$$

for the transformed ray after n round trips. This shows that both the position and the propagation direction of the ray at successive passages of the reference plane display a discrete oscillatory behavior. An interesting case arises when the Gouy phase χ is a rational fraction of 2π, i.e., if

$$\chi = \frac{2\pi K}{N} , \tag{2.15}$$

where K and N are integers. Then the two eigenvalues of M_{rt}^N are both equal to 1, so that $M_{\mathrm{rt}}^N = 1$. Inside a cavity this means that the trajectory of a ray will form a closed path after N round trips.

For a different choice of the reference plane, the round-trip ray matrix M_{rt} takes a different form. The two forms are related by a transformation determined by the ray matrix from one reference plane to the other. The same transformation also couples the eigenvectors. The eigenvalues, and therefore the notion of stability, are independent of the choice of the reference plane.

2.2.2 Two transverse dimensions

The description that we have discussed in the previous subsection can be generalized to optical set-ups with two independent transverse dimensions. In this case both the transverse position and the propagation direction of a ray become two-dimensional vectors. The transverse coordinates are denoted $\rho = (x, y)^{\mathrm{T}}$, and $\theta = (\vartheta_x, \vartheta_y)^{\mathrm{T}}$ are the angles that specify the propagation direction in the xz and yz planes. Likewise, the transformation from the input plane of an optical set-up to its output plane is represented by a 4×4 ray matrix, in the form

$$\begin{pmatrix} \rho_{\mathrm{out}} \\ \theta_{\mathrm{out}} \end{pmatrix} = M \begin{pmatrix} \rho_{\mathrm{in}} \\ \theta_{\mathrm{in}} \end{pmatrix} . \tag{2.16}$$

For an isotropic (non-astigmatic) optical element the 4×4 matrix is obtained by multiplying the four elements of the 2×2 ray matrix with a 2×2 unit matrix $\mathsf{1}$. For instance, the transformation for propagation through free space over a distance z can be expressed as

$$M_{\mathrm{f}}(z) = \begin{pmatrix} \mathsf{1} & z\mathsf{1} \\ \mathsf{0} & \mathsf{1} \end{pmatrix} , \tag{2.17}$$

where $\mathsf{0}$ is the 2×2 zero matrix. In case of an astigmatic optical element, at least some part of the ray matrix is not proportional to the identity matrix. For our present purposes, the most relevant example is that of an astigmatic thin lens. The ray matrix that describes its transformation can be written as

$$M_{\mathrm{l}}(\mathsf{F}) = \begin{pmatrix} \mathsf{1} & \mathsf{0} \\ -\mathsf{F}^{-1} & \mathsf{1} \end{pmatrix} , \tag{2.18}$$

where F is a real and symmetric 2×2 matrix. Its eigenvalues are the focal lengths of the lens, while the corresponding, mutually perpendicular, real eigenvectors fix the orientation of the lens in the transverse plane.

Again, the ray matrix that describes a composite optical system can be constructed by multiplying the ray matrices that describe the optical elements in the right order. In particular, the ray matrix that describes the transformation of a round trip through an astigmatic cavity can be obtained by unfolding the cavity into the corresponding lens guide and multiplying the matrices that represent the transformations of the different elements in the correct order

$$M_{\mathrm{rt}} = M_{\mathrm{l}}(\mathsf{F}_1) M_{\mathrm{f}}(L) M_{\mathrm{l}}(\mathsf{F}_2) M_{\mathrm{f}}(L) \ . \tag{2.19}$$

Here L is again the distance between the two mirrors and $\mathsf{F}_{1,2}$ are the matrices that describe the mirrors. If both mirrors have two equal focal lengths, i.e., if they are spherical, the cavity has cylinder symmetry. If one of the mirrors has two different focal lengths, i.e., is astigmatic, while the other is spherical or if both mirrors are astigmatic but with the same orientation, the cavity has two transverse symmetry directions and is said to have simple (or orthogonal) astigmatism. If this is not the case, i.e., if both mirrors are astigmatic and if they are in non-parallel alignment there are no transverse symmetry directions and the cavity has general (or non-orthogonal) astigmatism [18].

A typical ray matrix M is real, but not symmetric, so that its eigenvectors cannot be expected to be orthogonal. However, it is easy to check that the ray matrices (2.17) and (2.18) obey the identity

$$M^{\mathrm{T}} G M = G \tag{2.20}$$

where G is the anti-symmetric 4×4 matrix

$$G = \begin{pmatrix} \mathsf{0} & \mathsf{1} \\ -\mathsf{1} & \mathsf{0} \end{pmatrix} . \tag{2.21}$$

The same identity must hold for a composite optical set-up, in particular for the round-trip ray matrix M_{rt} (2.19). This is the defining property of a physical ray matrix that describes a lossless first-order optical system. It generalizes the defining properties of a 2×2 ray matrix to the astigmatic case. In mathematical terms, the above identity defines a symplectic group under matrix multiplication [39]. Physical ray matrices must be in the real symplectic group of 4×4 matrices, denoted as $Sp(4, \mathbb{R})$. The determinant of physical 4×4 ray matrices is equal to 1. It is noteworthy that the 2×2 analogue of equation (2.20) defines $Sp(2, \mathbb{R}) \cong SL(2, \mathbb{R})$.

From the general property (2.20) of the ray matrix (2.19) we can derive some important properties of its eigenvalues and eigenvectors. The eigenvalue relation is generally written as

$$M_{\mathrm{rt}} \mu_i = \lambda_i \mu_i \tag{2.22}$$

where μ_i are the four eigenvectors and λ_i are the corresponding eigenvalues. By taking matrix elements of the identity (2.20) between the eigenvectors, we find

$$\lambda_i \lambda_j \mu_i^{\mathrm{T}} G \mu_j = \mu_i^{\mathrm{T}} G \mu_j \ . \tag{2.23}$$

The matrix element $\mu_i^{\mathrm{T}} G \mu_i$ vanishes, so this relation gives no information on the eigenvalue for $i = j$. For different eigenvectors $\mu_i \neq \mu_j$, we conclude that either $\lambda_i \lambda_j = 1$, or $\mu_i^{\mathrm{T}} G \mu_j = 0$.

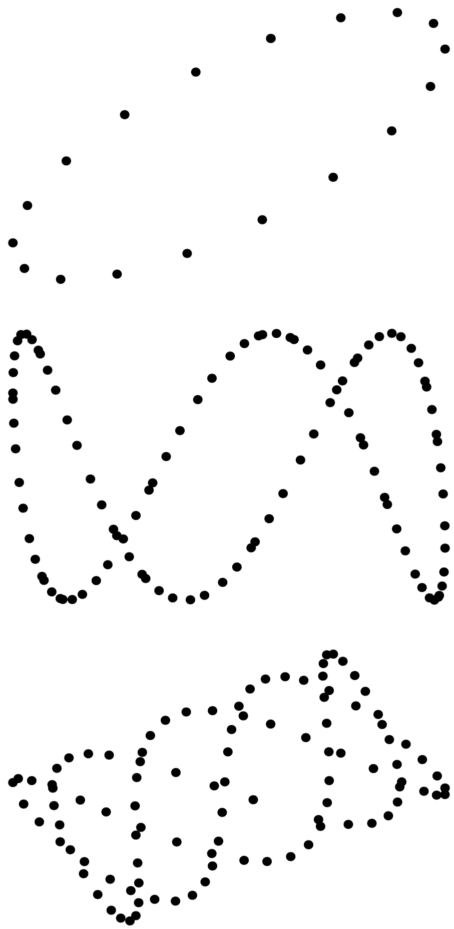

Figure 2.3: Hit points at a mirror of a ray in a cavity with degeneracy. The cavity has no astigmatism (above), simple astigmatism (middle) or general astigmatism (below). The cavity without astigmatism consists of two spherical mirrors with focal lengths $\simeq 1.08L$ and $\simeq 2.16L$. The cavity with simple astigmatism consists of two identical aligned astigmatic mirrors with focal lengths $\simeq 1.47L$ and $\simeq 2.94L$. The cavity with general astigmatism consists of two identical mirrors with focal lengths $\simeq 1.075L$ and $\simeq 2.15L$ which are rotated over an angle $\phi = \pi/3$ with respect to each other. In all cases the incoming ray is given by $r_0 = (1,\ 1.8,\ 3,\ 0.02)$.

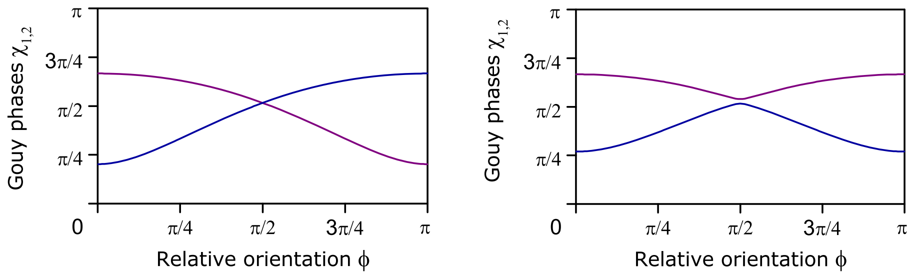

Figure 2.4: The dependence of the two Gouy phases on the relative orientation of two identical (left) and two slightly different (right) astigmatic mirrors. In the left window the mirrors are identical with focal lengths $f_\xi = L$ and $f_\eta = 10L$, with ξ and η indicating the principal axes of the mirrors. In the right figure the second mirror has focal lengths $f_\xi = L$ and $f_\eta = 4L$. Rotation angle $\phi = 0$ corresponds to the orientation for which the mirrors are aligned.

Since $M_{\rm rt}$ is real, when an eigenvalue λ_i is complex, the same is true for the eigenvector μ_i. Moreover, μ_i^* is an eigenvector of $M_{\rm rt}$ with eigenvalue λ_i^*. Provided that the matrix element $\mu_i^\dagger G \mu_i \neq 0$, the eigenvalue must then obey the relation $\lambda_i^* \lambda_i = 1$, so that the complex eigenvalue λ_i has absolute value 1. Just as in the case of one transverse dimension, stability requires that all eigenvalues have absolute value 1. Apart from accidental degeneracies, we conclude that a stable astigmatic cavity has two complex conjugate pairs of eigenvectors μ_1, μ_1^*, and μ_2, μ_2^* with eigenvalues λ_1, λ_1^*, and λ_2, λ_2^*, that can be written as

$$\lambda_1 = e^{i\chi_1} \qquad \text{and} \qquad \lambda_2 = e^{i\chi_2} \; . \tag{2.24}$$

Hence the eigenvalues now specify two different round-trip Gouy phases, and the complex eigenvectors obey the identities $\mu_1^{\rm T} G \mu_2 = 0$ and $\mu_1^\dagger G \mu_2 = 0$. On the other hand, the matrix elements $\mu_1^\dagger G \mu_1$ and $\mu_2^\dagger G \mu_2$ are usually nonzero. These matrix elements are purely imaginary, and without loss of generality we may assume that they are equal to the imaginary unit i times a positive real number. This can always be realized, when needed by interchanging μ_1 and μ_1^* (or μ_2 and μ_2^*), which is equivalent to a sign change of the matrix element. It is practical to normalize the eigenvectors, so that

$$\mu_1^\dagger G \mu_1 = \mu_2^\dagger G \mu_2 = 2i \; . \tag{2.25}$$

An arbitrary ray in the reference plane characterized by the real four-dimensional vector

$$z_0 = \begin{pmatrix} \rho \\ \theta \end{pmatrix} \tag{2.26}$$

can be expanded in the four complex basis vectors as

$$z_0 = 2\mathrm{Re}\,(a_1\mu_1 + a_2\mu_2) \;\; , \tag{2.27}$$

in terms of two complex coefficients a_1 and a_2. These coefficients can be obtained from a given ray vector r_0 by the identities

$$a_1 = \frac{\mu_1^\dagger G r_0}{2i} \qquad \text{and} \qquad a_2 = \frac{\mu_2^\dagger G r_0}{2i} \; . \tag{2.28}$$

This is obvious when one substitutes the expansion (2.27) in the right-hand sides of (2.28). After n round trips, the input ray (2.27) is transformed into the ray

$$r_n = M^n r_0 = 2\mathrm{Re}\left(a_1 \mu_1 e^{in\chi_1} + a_2 \mu_2 e^{in\chi_2}\right) \; . \tag{2.29}$$

This is a linear superposition of two oscillating terms that pick up a phase χ_1 and χ_2 respectively after each passage of the reference plane. When the two Gouy phases are rational fractions of 2π with a common denominator N, the ray path will be closed after N round trips. Then the cavity can be called degenerate. In this case the hit points of the ray on the mirrors (or in any transverse plane) lie on a well-defined closed curve. For a cavity that has no astigmatism this curve is an ellipse [12]. The transverse position and the propagation direction of the incoming ray determine the shape of the ellipse. In special (degenerate) cases it can reduce into a straight line or a circle. In case of a degenerate cavity with simple astigmatism the hit points lie on Lissajous curves [40, 41]. The ratio of the Gouy phases is equal to the ratio of the numbers of extrema of the curve in the two directions, while the incoming ray and the actual values of the Gouy phases determine its specific shape. The presence of general astigmatism gives rise to skew Lissajous curves, which are Lissajous curves in non-orthogonal coordinates. These properties are illustrated in figure 2.3.

The two round-trip Gouy phases of a cavity with two astigmatic mirrors depend on the relative orientation of the mirrors ϕ. When the cavity consists of two identical mirrors that are in parallel alignment, i.e., $\phi = 0$, it has simple astigmatism and the plane halfway between the mirrors is the focal plane for both components. Simple astigmatism also occurs for the anti-aligned configuration $\phi = \pi/2$, when the axis with the larger curvature of one mirror and the axis with the smaller curvature of the other one lie in a single plane through the optical axis. In this case both components necessarily have the same Gouy phase, and their foci lie symmetrically placed on opposite sides of the transverse plane halfway between the mirrors. The two Gouy phases attain extreme values for the aligned and the anti-aligned configuration. For intermediate orientations the cavity has general astigmatism, with Gouy phases varying between these extreme values. A crossing occurs in the anti-aligned geometry. The crossing is avoided when the mirrors are slightly different. The behavior of the Gouy phases as a function of the relative orientation ϕ is sketched in figure 2.4.

2.3 Paraxial wave optics

We describe the spatial structure of the modes in an astigmatic cavity in the same lens-guide picture that we used for the rays. The longitudinal coordinate in the lens guide is indicated by z, and $\rho = (x, y)^{\mathrm{T}}$ denotes the two-dimensional transverse position. A monochromatic beam of light with uniform polarization in the paraxial approximation is characterized by the expression

$$\mathbf{E}(\mathbf{r}, t) = \mathrm{Re}\left\{E_0 \epsilon u(\rho, z) e^{ikz - i\omega t}\right\} \tag{2.30}$$

for the transverse part of the electric field. It contains a carrier wave with wave number k and frequency $\omega = ck$, a normalized complex polarization vector ϵ and an amplitude E_0. The magnetic field is given by the analogous expression

$$\mathbf{B}(\mathbf{r}, t) = \frac{1}{c}\mathrm{Re}\left\{E_0(\mathbf{e}_z \times \epsilon) u(\rho, z) e^{ikz - i\omega t}\right\} , \tag{2.31}$$

where $\mathbf{e}_z$ is a unit vector along the propagation direction z. The transverse spatial structure of the beam for each transverse plane is determined by the normalized profile $u(\rho, z)$. During propagation in free space, the z dependence of the profile is governed by the paraxial wave equation

$$\left(\nabla_\rho^2 + 2ik\frac{\partial}{\partial z}\right) u(\rho, z) = 0 . \tag{2.32}$$

In a region of free propagation, the transverse profile $u(\rho, z)$ varies negligibly with z over a wavelength. On the other hand, u changes abruptly at the position of a thin lens. The effect of an astigmatic lens is given by the input-output relation for the beam profile [27]

$$u_{\mathrm{out}}(\rho) = \exp\left(-\frac{ik\rho^{\mathrm{T}} \mathsf{F}^{-1} \rho}{2}\right) u_{\mathrm{in}}(\rho) , \tag{2.33}$$

where the real symmetric matrix F specifies the orientation and the focal lengths of the lens. Again, an astigmatic lens in the lens guide models an equivalent astigmatic mirror in the cavity.

The paraxial wave equation (2.32) has the form of the Schrödinger equation for a free particle in two dimensions, where the longitudinal coordinate z plays the role of time. This analogy suggest to adopt the Dirac notation of quantum mechanics to describe the dynamics of classical light fields [42]. The beam profile is analogous to the particle wave function and we associate a profile state vector $|u(z)\rangle$ to it, so that

$$u(\rho, z) = \langle \rho | u(z) \rangle , \tag{2.34}$$

where $|\rho\rangle$ is an eigenstate of the transverse position operator $\hat{\rho} = (\hat{x}, \hat{y})^{\mathrm{T}}$. The canonically conjugate momentum operator is given by $k\hat{\theta} = -i\,(\partial/\partial x, \partial/\partial y)^{\mathrm{T}}$. The average (or expectation) value of this operator corresponds to the transverse momentum per photon in units of $\hbar$ [43]. The longitudinal momentum per photon equals $\hbar k$ and it follows that the operator $\hat{\theta}$ represents the ratio of the transverse and longitudinal momentum. Therefore, it corresponds to the local propagation direction in a beam and is the wave-optical analogue of the propagation direction θ of a ray. The components of $\hat{\rho}$ and $\hat{\theta}$ satisfy the canonical commutation relations

$$[\hat{x}, \hat{\vartheta}_x] = [\hat{y}, \hat{\vartheta}_y] = i\lambda\!\!\!^{-} , \tag{2.35}$$

where $\lambda = 1/k$. The effect of free propagation and of astigmatic lenses can be represented by unitary operators acting on the state vectors $|u\rangle$ in the Hilbert space of transverse modes. The paraxial wave equation (2.32) can be represented in operator notation as

$$\frac{d}{dz}|u(z)\rangle = -\frac{ik}{2}\hat{\theta}^2|u(z)\rangle \ . \tag{2.36}$$

Hence free propagation over a distance z has the effect

$$|u(z_0 + z)\rangle = \hat{U}_\mathrm{f}(z)|u(z_0)\rangle \tag{2.37}$$

with

$$\hat{U}_\mathrm{f}(z) = \exp\left(-\frac{ikz}{2}\hat{\theta}^2\right) \ , \tag{2.38}$$

while the effect of an astigmatic lens can be expressed as

$$|u_\mathrm{out}\rangle = \hat{U}_\mathrm{l}(\mathsf{F})|u_\mathrm{in}\rangle \tag{2.39}$$

with

$$\hat{U}_\mathrm{l}(\mathsf{F}) = \exp\left(-\frac{ik\hat{\rho}^\mathrm{T}\mathsf{F}^{-1}\hat{\rho}}{2}\right) \ . \tag{2.40}$$

The unitary transformation of an optical system can be constructed by multiplying the operators representing the elements in the proper order. Therefore, the unitary transformation describing a single round trip through the astigmatic cavity can be written as

$$\hat{U}_\mathrm{rt} = \hat{U}_\mathrm{l}(\mathsf{F}_1)\hat{U}_\mathrm{f}(L)\hat{U}_\mathrm{l}(\mathsf{F}_2)\hat{U}_\mathrm{f}(L) \ , \tag{2.41}$$

where the reference plane is the same as sketched in figure 2.2. It is clear that other unitary round-trip operators can be constructed for different reference planes. For different choices the operators are related by unitary transformations.

The variation of the position $\rho(z)$ and the direction $\theta(z)$ of a ray during propagation must be reproduced by the variation of the average value of $\hat{\rho}$ and $\hat{\theta}$ over the beam profile. Since the variation of this profile during propagation is governed by the evolution operator $\hat{U}(z)$, the propagation of a ray in geometric optics should be reproduced by the expectation value of $\hat{U}^\dagger\hat{\rho}\hat{U}$ and $\hat{U}^\dagger\hat{\theta}\hat{U}$, in analogy to the Heisenberg picture of quantum mechanics. Therefore, the wave-optical propagation operator $\hat{U}$ and the ray matrix M must be related by

$$\hat{U}^\dagger \begin{pmatrix} \hat{\rho} \\ \hat{\theta} \end{pmatrix} U = M \begin{pmatrix} \hat{\rho} \\ \hat{\theta} \end{pmatrix} \ . \tag{2.42}$$

One may check explicitly that this relation holds in the case of free propagation (described by $\hat{U}_\mathrm{f}$ and M_f) and for astigmatic lenses (described by $\hat{U}_\mathrm{l}$ and M_l). From this one verifies that the relation (2.42) must hold generally for any optical system that is composed of regions of free propagation, interrupted by astigmatic lenses (or mirrors).

It is noteworthy that the general property (2.20) of transfer matrices M can be reproduced by using this relation (2.42), combined with the fact that the Heisenberg-transformed operators $\hat{U}^\dagger\hat{\rho}\hat{U}$ and $\hat{U}^\dagger\hat{\theta}\hat{U}$ obey the canonical commutation rules (2.35).

2.4 Operator description of Gaussian modes

A characteristic of the paraxial wave equation is that a transverse beam profile with a Gaussian shape retains its Gaussian structure under propagation through free space. The same is true when the beam passes a thin lens (or a mirror) as described by the transformation of equation (2.40). The Gaussian shape is the general structure of a fundamental paraxial mode. The standard set of higher-order modes have the form of the same complex Gaussian multiplied by a Hermite polynomial in each of the transverse coordinates [12]. This provides the basis of Hermite-Gaussian modes, which can be rearranged to yield the basis of Laguerre-Gaussian modes. There is a clear similarity between these bases of paraxial optical modes and the stationary states of the isotropic quantum-mechanical harmonic oscillator in two dimensions. In analogy to the algebraic description of the harmonic oscillator, isotropic paraxial optical modes of different order can be connected by bosonic ladder operators [33]. In reference [17], it has been shown that the algebraic description of freely propagating paraxial modes can be generalized to account for general astigmatism.

Here, we show that the complete set of modes of a geometrically stable two-mirror cavity can be obtained from two pairs of bosonic ladder operators. These ladder operators are linear combinations of the position operator $\hat{\rho}$ and the propagation-direction operator $\hat{\theta}$ and can be expressed in terms of the eigenvectors of the round-trip ray matrix M_{rt}.

2.4.1 Gaussian modes in one transverse dimension

For simplicity, we first consider a single period of the lens guide that represents the cavity described in section 2.2, with one transverse dimension. In this case, the higher-order modes are obtained by repeated application of a raising operator $\hat{a}^{\dagger}$, acting on the fundamental mode. The raising operator is the Hermitian conjugate of the lowering operator, which can be expressed as

$$\hat{a}(z) = \sqrt{\frac{k}{2}} \left(r\hat{\vartheta} - t\hat{x} \right) , \tag{2.43}$$

where k is the wave number, and the z dependence of the ladder operators is determined only by the variation of the complex parameters r and t as a function of the longitudinal coordinate z. These parameters also determine the z dependent profile of the fundamental mode

$$u_0(x,z) = \left(\frac{k}{r^2\pi} \right)^{1/4} \exp\left(\frac{iktx^2}{2r} \right) \equiv \left(\frac{k}{r^2\pi} \right)^{1/4} \exp\left(-\frac{ksx^2}{2} \right) , \tag{2.44}$$

where $s = -it/r$. The parameters r, t and s have been defined such that they have a purely geometric significance, in that they are fully determined by the geometric properties of the cavity, the length L, and the focal lengths $f_{1,2}$, independent of k. They determine the transverse beam width and the radius of curvature of the wave front according to $w = \sqrt{2/(ks_{\mathrm{r}})}$ and $R = 1/s_{\mathrm{i}}$, where s_{r} and s_{i} are respectively the real and imaginary parts of s.

For each value of z, the ladder operators $\hat{a}$ and $\hat{a}^\dagger$ must obey the bosonic commutation rule

$$[\hat{a}(z), \hat{a}^\dagger(z)] = 1 \; , \tag{2.45}$$

which requires that r and t obey the normalization identity

$$r^* t - t^* r = 2i \; . \tag{2.46}$$

With this condition, the fundamental mode profile (2.44) is normalized, in the sense that $\int dx |u(x,z)|^2 = 1$ for all values of z. Moreover, the lowering operator (2.43) gives zero when acting on the fundamental mode (2.44), so that $\hat{a}(z)|u_0(z)\rangle = 0$.

The z dependent propagation operator $\hat{U}(z)$ is defined to transform the beam profile in the reference plane at $z = 0$ of the lens guide into the profile in another transverse plane at position z. Then $|u(z)\rangle = \hat{U}(z)|u(0)\rangle$ describes a light beam propagating through the optical system. This means that in the regions of free propagation between the lenses, $|u(z)\rangle$ solves the paraxial wave equation (2.32), while it picks up the appropriate phase factor when passing through a lens. The z dependence of the parameters r and t must be chosen in such a way that the ladder operators $\hat{a}(z)$ and $\hat{a}^\dagger(z)$ acting on a z dependent mode $|u(z)\rangle$ create another mode that solves the wave equation. This condition can be summarized as

$$\hat{a}(z)|u(z)\rangle = \hat{U}(z)\hat{a}(0)|u(0)\rangle \; , \tag{2.47}$$

which, in view of the unitarity of the propagation operator, is equivalent to the operator identity

$$\hat{a}(z) = \hat{U}(z)\hat{a}(0)\hat{U}^\dagger(z) \; . \tag{2.48}$$

When this is the case, a complete orthogonal set of higher-order modes is obtained in terms of the raising operator and the fundamental mode, in the well-known form

$$|u_n(z)\rangle = \frac{1}{\sqrt{n!}}\left(\hat{a}^\dagger(z)\right)^n |u_0(z)\rangle \; . \tag{2.49}$$

In reference [33], it has been shown that the transformation (2.48) of the lowering operator (2.43) under free propagation, as described by the transformation in equation (2.38), implies that the parameter t is constant in a region of free propagation, while r has the derivative $dr/dz = t$. Upon passage through a lens with focal length f, as described by the transformation in equation (2.40), r does not change, whereas t modifies according to the relation $t_{\text{out}} = t_{\text{in}} - r/f$. This z dependence of the parameters can be summarized by the statement that the transformation of the two-dimensional vector $(r,t)^{\mathrm{T}}$ during propagation is identical to the transformation of a ray $(x,\vartheta)^{\mathrm{T}}$. This transformation is described by the ray matrix $M(z)$ that corresponds to $\hat{U}(z)$ in accordance with equation (2.42), so that

$$\begin{pmatrix} r(z) \\ t(z) \end{pmatrix} = M(z) \begin{pmatrix} r(0) \\ t(0) \end{pmatrix} \; . \tag{2.50}$$

Now it is straightforward to obtain the modes and the eigenfrequencies of the cavity. The condition for a mode is that the mode profile $u(x,z)$ reproduces after a round trip, up to a phase factor. This is accomplished when the two-dimensional vector $(r(0),t(0))^{\mathrm{T}} = \mu$ is an eigenvector of the round-trip ray matrix $M_{\mathrm{rt}} = M(2L)$, after proper normalization of μ to ensure that r and t obey the identity (2.46). (In the case that $r^*t - t^*r$ turns out to be a negative imaginary number, we just take the other eigenvector μ^* instead of μ.) With this choice, the fundamental mode obeys the relation $|u_0(2L)\rangle = \exp(-i\chi/2)|u_0(0)\rangle$, and the lowering operator transforms after a round trip as $\hat{a}(2L) = \exp(i\chi)\hat{a}(0)$, with χ the round-trip Gouy phase. The n^{th}-order mode (2.49) then obeys the well-known relation

$$|u_n(2L)\rangle = e^{-i(n+1/2)\chi}|u_n(0)\rangle \ . \tag{2.51}$$

As indicated in equation (2.30), the complex electric field, which should reproduce exactly after a round trip, is proportional to $u_n(x,z)\exp(ikz)$, so that the resonance condition reads

$$2kL - \left(n + \frac{1}{2}\right)\chi = 2\pi q \ , \tag{2.52}$$

where $q \in \mathbb{Z}$ plays the role of the longitudinal mode number. This relation defines the frequencies of the cavity modes $\omega = ck$.

In conclusion, we have shown that the cavity modes are determined by the values of the parameters r and t, such that in the reference plane the vector $(r(0),t(0))^{\mathrm{T}}$ is equal to the normalized eigenvector μ of the round-trip ray matrix M_{rt}. The z dependence of the parameters $r(z)$ and $t(z)$ is governed by the ray matrix that connects the reference plane $z = 0$ in the lens guide to another transverse plane z. This is equivalent to the statement that the vector $(r(z),t(z))^{\mathrm{T}}$ coincides with the eigenvector of the ray matrix for a round trip starting in the transverse plane z. Different modes of the cavity take a different form and have different wave numbers k, but they are all characterized by the same complex parameters r and t.

Before turning to the case of two transverse dimensions, it is illuminating to relate the z dependence of the ladder operators to their structure in terms of the matrix G. In the present case of one transverse dimension, this matrix as defined in (2.21) is two-dimensional, just as the vectors $(r,t)^{\mathrm{T}}$ and $(x,\vartheta)^{\mathrm{T}}$. Then the property (2.20) of M_{rt} is just equivalent to the statement that $\det M_{\mathrm{rt}} = 1$. Also for a single transverse dimension the ray matrix M_{rt} is linked to the propagation operator $\hat{U}_{\mathrm{rt}}$ by the identity (2.42). We can rewrite the expression (2.43) for the lowering operator as

$$\hat{a}(z) = \sqrt{\frac{k}{2}}(r(z),t(z))G\begin{pmatrix} \hat{x} \\ \hat{\vartheta} \end{pmatrix} . \tag{2.53}$$

When we substitute this expression in the transformation rule (2.47) for $\hat{a}$, while using the two-dimensional version of the relation (2.42), we obtain

$$\hat{a}(z) = \sqrt{\frac{k}{2}}(r(0),t(0))M^{\mathrm{T}}(z)G\begin{pmatrix} \hat{x} \\ \hat{\vartheta} \end{pmatrix} , \tag{2.54}$$

where we used the identity (2.20) in the form $GM^{-1} = M^{\mathrm{T}}G$. The equivalence of (2.53) and (2.54) is in obvious accordance with the identity (2.50).

2.4.2 Astigmatic Gaussian modes

The formulation that we have given for the modes in one transverse dimension allows a direct generalization to two transverse dimensions. In that case we must have two lowering operators rather than one. Since these operators must return to their initial form after a full round trip, they must be determined by the eigenvectors of the round-trip ray matrix M_{rt}. In analogy to the expression (2.53), we introduce the two z dependent lowering operators

$$\hat{a}_i(z) = \sqrt{\frac{k}{2}}\mu_i^{\mathrm{T}} M^{\mathrm{T}}(z) G \begin{pmatrix} \hat{\rho} \\ \hat{\theta} \end{pmatrix} , \tag{2.55}$$

in terms of the two eigenvectors μ_i of M_{rt} with $i = 1, 2$. By the same argument as given for equation (2.54), these operators obey the transformation rule (2.48), and in the reference plane at $z = 0$ they are given by

$$\hat{a}_i(0) = \sqrt{\frac{k}{2}}\mu_i^{\mathrm{T}} G \begin{pmatrix} \hat{\rho} \\ \hat{\theta} \end{pmatrix} . \tag{2.56}$$

Over a full round trip, they transform as

$$\hat{a}_i(2L) = e^{i\chi_i}\hat{a}_i(0) , \tag{2.57}$$

in terms of the eigenvalues (2.24) corresponding to μ_i. By using the identities (2.25), one verifies that the ladder operators obey the commutation rules

$$[\hat{a}_i(z), \hat{a}_i^{\dagger}(z)] = 1 . \tag{2.58}$$

By using the identities $\mu_1^{\dagger} G \mu_2 = \mu_1^{\mathrm{T}} G \mu_2 = 0$, we find that other commutators vanish, so that $[\hat{a}_2, \hat{a}_1^{\dagger}] = [\hat{a}_2, \hat{a}_1] = 0$. For notational convenience we combine the two lowering operators into a vector of operators

$$\hat{A} = \begin{pmatrix} \hat{a}_1 \\ \hat{a}_2 \end{pmatrix} , \tag{2.59}$$

for all values of z. In analogy to equation (2.43), this can be written as

$$\hat{A} = \sqrt{\frac{k}{2}} \left(\mathsf{R}^{\mathrm{T}}\hat{\theta} - \mathsf{T}^{\mathrm{T}}\hat{\rho} \right) , \tag{2.60}$$

where now R and T are z dependent 2×2 matrices. Comparison with equation (2.55) shows that in the reference plane $z = 0$ the two matrices $\mathsf{R}^{\mathrm{T}}(0)$ and $\mathsf{T}^{\mathrm{T}}(0)$ can be combined into a single 2×4 matrix, where the two rows coincide with the transposed eigenvectors μ_i^{T}. This gives the formal identification

$$\begin{pmatrix} \mathsf{R}(0) \\ \mathsf{T}(0) \end{pmatrix} = (\mu_1 \; \mu_2) . \tag{2.61}$$

Equation (2.60) then shows that the z dependence of R and T can formally be expressed as

$$\begin{pmatrix} \mathsf{R}(z) \\ \mathsf{T}(z) \end{pmatrix} = M(z) \begin{pmatrix} \mathsf{R}(0) \\ \mathsf{T}(0) \end{pmatrix} , \tag{2.62}$$

where in the right-hand side a 4×4 matrix multiplies a 4×2 matrix, producing a 4×2 matrix. The behavior of M as a function of z is fully determined by the expressions (2.17) and (2.18) for free propagation and at passage of a lens. It follows that during free propagation, T is constant, while R obeys the differential equation $d\mathsf{R}/dz = \mathsf{T}$. At passage through a lens with focal matrix F, R does not change, whereas the change in T is given by

$$\mathsf{T}_{\text{out}} = \mathsf{T}_{\text{in}} - \mathsf{F}^{-1}\mathsf{R} . \tag{2.63}$$

The fundamental mode $|u_{00}(z)\rangle$ in the astigmatic cavity is defined by the requirement that it obeys the paraxial wave equation, and that it gives zero when acted on with the lowering operators $\hat{a}_i$. It is easy to check that these conditions are obeyed by the normalized mode function

$$u_{00}(\rho, z) = \sqrt{\frac{k}{\pi \det \mathsf{R}}} \exp\left(\frac{ik\rho^{\mathrm{T}}\mathsf{T}\mathsf{R}^{-1}\rho}{2}\right) \equiv \sqrt{\frac{k}{\pi \det \mathsf{R}}} \exp\left(-\frac{k\rho^{\mathrm{T}}\mathsf{S}\rho}{2}\right) \tag{2.64}$$

in terms of the z dependent matrices R and T. The matrix $\mathsf{S} = -i\mathsf{T}\mathsf{R}^{-1}$ is symmetric and its real part S_{r} is positive definite, as can be checked by using the properties of the eigenvectors μ_i derived in section 2.2. Because of the definitions of R and T in terms of the eigenvectors of the round-trip ray matrix M_{rt}, the fundamental mode returns to itself after a round trip, as expressed by

$$|u_{00}(2L)\rangle = e^{-i(\chi_1+\chi_2)/2}|u_{00}(0)\rangle . \tag{2.65}$$

Higher-order modes are defined by repeated application of the raising operators, which gives

$$|u_{nm}(z)\rangle = \frac{1}{\sqrt{n!m!}} \left(\hat{a}_1^\dagger(z)\right)^n \left(\hat{a}_2^\dagger(z)\right)^m |u_{00}(z)\rangle . \tag{2.66}$$

The set of modes functions $|u_{nm}(z)\rangle$ is complete and orthonormal in each transverse plane. Because of the round-trip properties (2.57) of the ladder operators, the modes transform over a round trip as

$$|u_{nm}(2L)\rangle = e^{-i(n+1/2)\chi_1 - i(m+1/2)\chi_2}|u_{nm}(0)\rangle . \tag{2.67}$$

The requirement that the electric field of a mode, which is proportional to $u_{nm}(\rho, z)\exp(ikz)$, picks up a phase that is a multiple of 2π, gives the resonance condition for the wave number

$$2kL - \left(n + \frac{1}{2}\right)\chi_1 - \left(m + \frac{1}{2}\right)\chi_2 = 2\pi q , \tag{2.68}$$

so that the frequency of the mode specified by the transverse mode numbers n and m, and the longitudinal mode number q is

$$\omega = \frac{c}{2L}\left\{2\pi q + \left(n + \frac{1}{2}\right)\chi_1 + \left(m + \frac{1}{2}\right)\chi_2\right\} . \tag{2.69}$$

Apparently, the general astigmatism does not show up in the frequency spectrum of the cavity. All that can be seen is the presence of two different round-trip Gouy phases. There are two different ways in which the corresponding frequency spectrum can be degenerate. For a cavity that has cylinder symmetry the two eigenvalue spectrum of the ray matrix is degenerate (i.e., $\chi_1 = \chi_2$) and its modes are frequency degenerate in the total mode number $n + m$. As a result any linear combination of modes with the same total mode number is a mode too. The second kind of degeneracy arises when one of the Gouy phases is a rational fraction of 2π. Then the combs of modes at different values of q overlap so that many different modes appear at the same frequency.

2.5 Physical properties of the cavity modes

2.5.1 Symmetry properties

So far we have described the modes as a periodic solution of the paraxial equation in the lens guide that is equivalent to the cavity. The electric and magnetic field in the cavity are obtained by refolding the periodic lens-guide fields (2.30) and (2.31). The fields in two successive intervals with length L in the lens guide then give the fields propagating back and forth inside the cavity. The electric field (2.30) in the lens guide then gives the expression for the field in the cavity

$$\mathbf{E}_{\text{cavity}}(\mathbf{r}, t) = \operatorname{Re}\left\{E_0 \epsilon f(\rho, z) i e^{-i\omega t}\right\} \tag{2.70}$$

for $0 < z < L$, with

$$f(\rho, z) = \frac{1}{i}\left\{u(\rho, z)e^{ikz} - u(\rho, -z)e^{-ikz}\right\} \ . \tag{2.71}$$

The minus sign in (2.71) ensures that the mirror surfaces coincide with a nodal plane. This follows from the relation (2.63) between the input and the output of a lens. Applied to the lens at $z = 0$, this shows that in the lens guide the transverse profile $u(\rho, 0^{\pm})$ just left and right of lens 1 can be written as

$$u(\rho, 0^{\pm}) = u_1(\rho) \exp\left(\mp \frac{ik\rho^{\mathrm{T}} \mathsf{F}_1^{-1} \rho}{4}\right) , \tag{2.72}$$

where u_1 may be viewed as the transverse profile halfway lens 1. Substitution in equation (2.71) shows that the cavity field f near mirror 1 is given by $2u_1(\rho) \sin\left(kz - k\rho^{\mathrm{T}} \mathsf{F}_1^{-1} \rho/4\right)$. Since the value of k obeys the resonance condition (2.68), which makes $u(\rho, z)\exp(ikz)$ periodic, a similar argument holds for mirror 2. When $u_2(\rho)$ is defined as the periodic lens-guide field $u(\rho, z)\exp(ikz)$ at the plane halfway lens 2, the cavity field f near mirror 2 (where $z \approx L$) is $2u_2(\rho) \sin\left(k(z - L + k\rho^{\mathrm{T}} \mathsf{F}_2^{-1} \rho/4)\right)$.

The corresponding expression for the magnetic field in the cavity is

$$\mathbf{B}_{\text{cavity}}(\mathbf{r}, t) = \operatorname{Re}\left\{E_0(\mathbf{e}_z \times \epsilon) b(\rho, z) e^{-i\omega t}\right\} , \tag{2.73}$$

with

$$b(\rho, z) = \frac{1}{c}\left\{u(\rho, z)e^{ikz} + u(\rho, -z)e^{-ikz}\right\} , \tag{2.74}$$

for $0 < z < L$. The expression (2.74) for the magnetic field has a plus sign, arising from the fact that the propagation direction $\mathbf{e}_z$ in (2.31) is replaced by $-\mathbf{e}_z$ for the field component propagating in the negative direction. Near mirror 1, the magnetic field function b is given by $2u_1(\rho)\cos\left(kz - k\rho^{\mathrm{T}}\mathsf{F}_1^{-1}\rho/4\right)/c$, while near mirror 2 we find $b(\rho, z) = 2u_2(\rho)\cos\left(k(z - L + k\rho^{\mathrm{T}}\mathsf{F}_2^{-1}\rho/4)\right)/c$.

The paraxial field in the cavity as described here arises from refolding a periodic field in the lens guide that propagates in the positive direction. We could just as well start from a lens guide field propagating in the negative z direction. Such a field is obtained by replacing $u(\rho, z)\exp(ikz)$ by its complex conjugate in equation (2.30). This leads to an alternative expression for the cavity field in the form (2.70) with f given by $[u^*(\rho, z)\exp(-ikz) - u^*(\rho, -z)\exp(ikz)]/i$. For a non-degenerate mode, this alternative expression for f must be proportional to the expression (2.71). This leads to the symmetry relation

$$u(\rho, -z) = u^*(\rho, z) , \tag{2.75}$$

apart from an overall phase factor. This shows that the mode functions $f(\rho, z)$ and $b(\rho, z)$ are real, so that they can be expressed as

$$f(\rho, z) = 2\,\mathrm{Im}\left\{u(\rho, z)e^{ikz}\right\} \qquad \text{and} \qquad b(\rho, z) = \frac{2}{c}\,\mathrm{Re}\left\{u(\rho, z)e^{ikz}\right\} . \tag{2.76}$$

From equations (2.70) and (2.73) we find that in a non-degenerate paraxial mode of a two-mirror cavity the electric and the magnetic field can be written as

$$\mathbf{E}_{\mathrm{cavity}}(\mathbf{r}, t) = -f(\rho, z)\mathrm{Im}\left\{E_0\epsilon e^{-i\omega t}\right\} \tag{2.77}$$

and

$$\mathbf{B}_{\mathrm{cavity}}(\mathbf{r}, t) = b(\rho, z)\mathrm{Re}\left\{E_0(\mathbf{e}_z \times \epsilon)e^{-i\omega t}\right\} , \tag{2.78}$$

which are products of a real function of position and a real function of time. Both fields take the form of a standing wave, with phase difference $\pi/2$. The curved transverse nodal planes of the electric field are determined by the requirement that $u(\rho, z)\exp(ikz)$ is real. These nodal planes coincide with the antinodal planes of the magnetic field.

2.5.2 Shape of the modes

It is interesting to notice that the real and the imaginary part of the complex propagating field in the lens guide correspond to the electric and magnetic field in the cavity, as given by the expression

$$u(\rho, z)e^{ikz} = cb(\rho, z) + if(\rho, z) . \tag{2.79}$$

This shows that the nodal planes of the electric or the magnetic field in the cavity are wavefronts of the traveling wave in the lens guide.

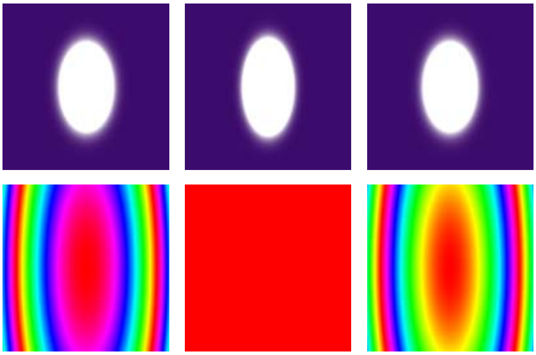

Figure 2.5: Intensity (top) and false-color phase (bottom) patterns of the fundamental mode of a lens guide with simple astigmatism. The corresponding cavity consists of two identical astigmatic mirrors with focal lengths $f_\xi = L$ and $f_\eta = 10L$, where L is the mirror separation. The ξ and η directions of the mirrors are aligned along the horizontal and vertical directions. From left to right the plots show the mode structure close to mirror 1, in the transverse plane in between the mirrors and close to mirror 2. The color code used to plot the phase patterns is periodic; from 0 to 2π the color changes in a continuous fashion from red via yellow, green, blue and purple back to red.

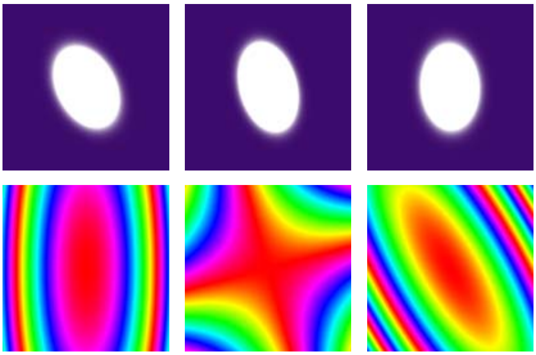

Figure 2.6: Intensity (top) and false-color phase (bottom) patterns of the fundamental mode of a lens guide with general astigmatism. The corresponding cavity consists of two identical astigmatic mirrors with focal lengths $f_\xi = L$ and $f_\eta = 10L$, where L is the mirror separation. Compared to the plots in figure 2.5, the right mirror is rotated over $\pi/6$ in the positive (counterclockwise) direction. From left to right the plots show the mode structure close to mirror 1, in the transverse plane in between the mirrors and close to mirror 2. The color code used to plot the phase patterns is periodic; from 0 to 2π the color changes in a continuous fashion from red via yellow, green, blue and purple back to red.

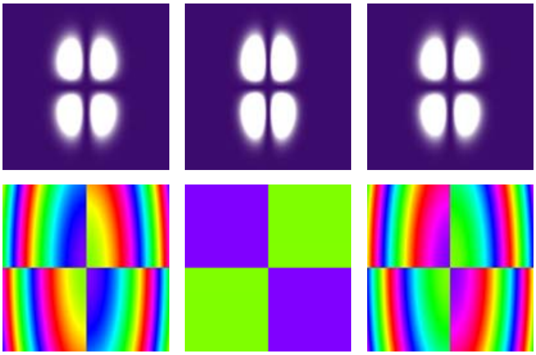

Figure 2.7: Intensity (top) and false-color phase (bottom) patterns of the $(1, 1)$ mode of a lens guide with simple astigmatism. The corresponding cavity consists of two identical astigmatic mirrors with focal lengths $f_\xi = L$ and $f_\eta = 10L$, where L is the mirror separation. The ξ and η directions of the mirrors are aligned along the horizontal and vertical directions. From left to right the plots show the mode structure close to mirror 1, in the transverse plane in between the mirrors and close to mirror 2. The color code used to plot the phase patterns is periodic; from 0 to 2π the color changes in a continuous fashion from red via yellow, green, blue and purple back to red.

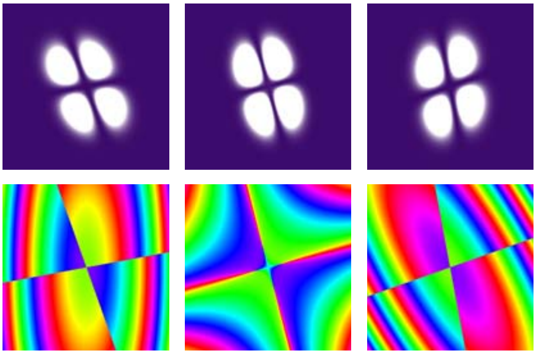

Figure 2.8: Intensity (top) and false-color phase (bottom) patterns of the $(1, 1)$ mode of a lens guide with general astigmatism. The corresponding cavity consists of two identical astigmatic mirrors with focal lengths $f_\xi = L$ and $f_\eta = 10L$, where L is the mirror separation. Compared to the plots in figure 2.7, the right mirror is rotated over $\pi/6$ in the positive (counterclockwise) direction. From left to right the plots show the mode structure close to mirror 1, in the transverse plane in between the mirrors and close to mirror 2. The color code used to plot the phase patterns is periodic; from 0 to 2π the color changes in a continuous fashion from red via yellow, green, blue and purple back to red.

From the symmetry property (2.75) it follows that the periodic lens-guide field $u(\rho, z)\exp(ikz)$ is real in the transverse plane halfway each of the lenses. Since this conclusion holds for modes of all orders, also the ladder operators $\hat{a}_i$ can be chosen real in these two symmetry planes. As a result, the higher-order modes have the nature of astigmatic Hermite-Gaussian modes, with a pattern of two sets of parallel straight nodal lines. However, nodal lines in these two sets are not orthogonal in the case of a twisted cavity.

In the free space between the mirrors of a twisted cavity the modes attain a structure with vortices, arising from an elliptical rather than a linear nature of the distribution of transverse momentum. Only in the special case of simple astigmatism, the modes have a Hermite-Gaussian structure in all transverse planes, with rectangular patterns of nodal lines that are aligned to the axes of the two mirrors.

2.5.3 Orbital angular momentum

As a result of the twisted boundary conditions that are imposed by two astigmatic mirrors in non-parallel alignment, the cavity modes become twisted as well. Both the elliptical intensity distribution of the fundamental cavity mode as well as its elliptical or hyperbolic curves of constant phase change their orientation under propagation from one mirror to the other. This tumbling gives rise to orbital angular momentum in the cavity modes [17]. In the higher-order modes both the general astigmatism and the vortices, which appear in intermediate transverse planes, contribute to the orbital angular momentum [16].

The leading-order contribution to the orbital angular momentum per unit length in a monochromatic paraxial beam, as characterized by equations (2.30) and (2.31), is longitudinal. Its z component can be expressed as [43, 6]

$$\mathcal{L} = \frac{\epsilon_0 |E_0|^2}{2i\omega} \int d_2\rho \; u^*(\rho, z, t) \left(x\frac{\partial}{\partial y} - y\frac{\partial}{\partial x} \right) u(\rho, z, t) \; . \tag{2.80}$$

In terms of the transverse position and momentum operators this can be rewritten as $N\hbar\langle u(z)| \hat{\rho} \times k\hat{\theta} |u(z)\rangle$, where $N = \epsilon_0 |E_0|^2/(2\hbar\omega)$ is the number of photons per unit length and $\times$ denotes a cross product in the transverse plane. By the virtue of equation (2.60) and its hermitian conjugate, the canonical operators $\hat{\rho}$ and $\hat{\theta}$ can be expressed in terms of the ladder operators $\hat{A}$ and $\hat{A}^\dagger$. This leads to an expression for the orbital angular momentum in the (n, m) cavity mode in terms of the vectors $r_{1,2}(0)$ and $t_{1,2}(0)$. It can be cast in the following form

$$\begin{aligned} \mathcal{L}_{nm} &= N\hbar\langle u_{nm}(z)|\hat{\rho} \times k\hat{\theta}|u_{nm}(z)\rangle = \\ &N\hbar\left\{ \left(n + \frac{1}{2}\right) \mathrm{Re}(r_1^*(0) \times t_1(0)) + \left(m + \frac{1}{2}\right) \mathrm{Re}(r_2^*(0) \times t_2(0)) \right\} . \end{aligned} \tag{2.81}$$

This very natural expression of the orbital angular momentum clearly shows its origin in the geometry of the twisted cavity. In terms of the eigenvectors μ_1 and μ_2, it may be rewritten as

$$\mathcal{L}_{nm} = N\hbar\left\{ \left(n + \frac{1}{2}\right) \frac{\mu_1^\dagger G J \mu_1}{2} + \left(m + \frac{1}{2}\right) \frac{\mu_2^\dagger G J \mu_2}{2} \right\} , \tag{2.82}$$

where

$$J = \begin{pmatrix} 0 & 1 & 0 & 0 \\ -1 & 0 & 0 & 0 \\ 0 & 0 & 0 & 1 \\ 0 & 0 & -1 & 0 \end{pmatrix} \tag{2.83}$$

is the generator of rotations of a ray (ρ, θ) in the transverse plane, i.e., $M_{\mathrm{rot}}(\alpha) = e^{-\alpha J}$ is the ray matrix $\in Sp(4, \mathbb{R})$ that rotates both the transverse position and the propagation direction of a ray over an angle α. From the fact that the ray matrix for free propagation (2.17) commutes with J, it is clear that the orbital angular momentum in the cavity modes is conserved under free propagation from one mirror to the other. Since the lens-guide mode profiles close to the lenses are real apart from the curved wave fronts, which locally fit on the mirror surfaces, it follows that they are converted into their complex conjugates when passing a lens. As a result, the orbital angular momentum in the cavity mode changes sign when the beam passes a lens (mirror) so that there is no net orbital angular momentum in the cavity field as characterized by equations (2.70) and (2.73).

2.6 Examples

We illustrate the intensity and phase structure and the orbital angular momentum of twisted cavity modes by investigating a specific example. We consider a cavity that consists of two identical astigmatic mirrors with focal lengths $f_\xi = L$ and $f_\eta = 10L$, where L is the mirror separation. The cavity has simple astigmatism when the mirrors are in parallel (or anti-parallel) alignment whereas it has general astigmatism when they are non-aligned. It is geometrically stable for all (relative) orientations of the mirrors.

2.6.1 Mode structure

It is convenient to plot the intensity and phase patterns in the corresponding lens guide. In figures 2.5 and 2.6, we show the transverse intensity and phase patterns of the fundamental lens-guide mode both in the immediate neighborhood of the lenses (mirrors) and in the transverse plane between them. The plots in figure 2.5 correspond to the case in which the ξ and η directions of the mirrors are aligned along the horizontal and vertical directions. In this case, the cavity has transverse symmetry directions along the axes of the mirrors. The elliptical intensity patterns of the fundamental mode are aligned along these symmetry directions. Since the mirrors have different radii of curvature along their axes, the diffraction of the mode is (slightly) different for the two directions so that the ellipticity of the curves of constant intensity varies under propagation from one lens to the other. The phase patterns close to the mirrors confirm that the wave fronts of the lens-guide mode fit on the mirror surfaces. Since the cavity mirrors are identical, the lens guide has an additional inversion-symmetry plane in between the lenses (mirrors). As a result, this plane is the focal plane of the lens-guide modes

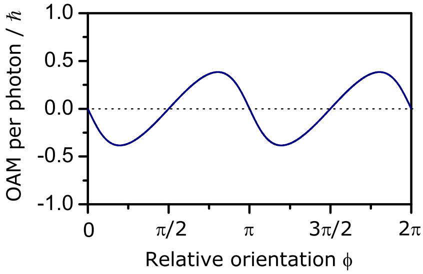

Figure 2.9: Orbital angular momentum in the (1, 1) mode of a lens guide corresponding to a cavity with two identical astigmatic mirrors as a function of the relative orientation of the mirrors. The mirrors have focal lengths $f_\xi = L$ and $f_\eta = 10L$, where L is the mirror separation and $\phi = 0$ corresponds to the case in which the mirrors are aligned.

so that the wave fronts of the fundamental mode in the immediate neighborhood of this plane are flat.

The plots in figure 2.6 show the fundamental lens-guide mode in the case in which the right mirror is rotated over $\pi/6$ in the positive (counterclockwise) direction. This obviously introduces a twist in the mode. The wave fronts close to the lenses (mirrors) fit on the lenses (mirrors) while the orientation of the ellipses of constant intensity reflects their non-parallel alignment. As a result of the twist, the inversion symmetry in the transverse plane between the lenses is broken and the focal planes for the two transverse components do not coincide. In between the focal planes, the lines of constant phase are hyperbolas rather than ellipses.

As an example of a higher-order mode, we show the intensity and phase patterns of the (1, 1) lens-guide mode. The plots in figure 2.7 show the intensity and phase patterns of the (1, 1) mode in the case in which the mirrors are aligned. The mode is aligned along the mirror axes and, although propagation from one lens to the other does affect the scaling of the mode pattern along the symmetry axes, propagation does not affect its orientation. The mode takes the form of a Hermite-Gaussian in all transverse planes, which has two mutually perpendicular lines of zero intensity (line dislocations) in the transverse plane. Up to phase jumps of π, which are due to the dislocations, the phase structure in the immediate neighborhood of the lenses reflects the shape of the mirrors. The plots in figure 2.8 show how the phase and intensity patterns of the (1, 1) mode change when the cavity is twisted. In this case, the intensity patterns close to the mirrors are not aligned along the mirror axes and the lines of zero intensity are no longer mutually perpendicular. The orientation of both the phase and the intensity patterns as well as the orientation of the line dislocations change upon propagation from one mirror to the other. Moreover, the mode is Hermite-Gaussian only in the immediate neighborhood of the lenses. In other transverse planes, it takes the form of a generalized Gaussian mode [44] and has elliptical vortices, rather than line dislocations, in the transverse plane. These are visible in the middle plots in figure 2.8.

2.6.2 Orbital angular momentum

The amount of orbital angular momentum in twisted cavity modes depends on the (relative) orientation of the mirrors. If the mirrors are in parallel or anti-parallel alignment, the cavity has simple astigmatism so that the orbital angular momentum vanishes. For intermediate orientations, the lens-guide modes do contain orbital angular momentum. A typical example of its dependence on the relative orientation of the mirrors is shown in figure 2.9. As was mentioned already, there is no net orbital angular momentum in the corresponding cavity field. The cavity mirrors invert the orbital angular momentum while reflecting the light, which implies that they experience a torque. This torque on mirror 2 amounts to $2c\mathcal{L}_{nm}$ while mirror 1 experiences the opposite torque. If the mirrors were allowed to rotate freely, the configurations with simple astigmatism (and therefore vanishing OAM) could either be stable or metastable. If $\mathcal{L}_{nm}$ goes through zero with a negative slope as a function of the orientation of mirror 2, the OAM of the modes gives rise to a torque that tends to restore the configuration. If $\mathcal{L}_{nm}$ goes through zero with a positive slope it is the other way around. The results shown in figure 2.9 indicate that the configuration that combines the largest and smallest radii of curvature is the stable one.

2.7 Discussion and conclusions

We have presented an algebraic method to obtain the complete and orthonormal set of paraxial modes of a geometrically stable two-mirror cavity with astigmatism. If the axes of the two mirrors are parallel, the modes take a factorized form and the problem of finding them is equivalent to the case of a single transverse dimension. In that case standard analytical techniques suffice to find expressions of the cavity modes. Finding expressions of the cavity modes is considerably more complex when the astigmatic mirror are non-parallel. In that case, the mode fields propagating between the mirrors display general astigmatism and no simple analytical approach is known to solve the problem of finding them.

An essential ingredient in our characterization of the cavity modes is the real 4×4 ray matrix M_{rt}, which is a purely geometric concept from ray optics and describes the transformation of a ray over one round trip through the cavity. We have argued that a cavity is geometrically stable only if the absolute values of all four eigenvalues of the round-trip ray matrix M_{rt} are equal to 1. Because of the special (group-theoretical) properties of the round-trip ray matrix, the requirement of geometric stability implies that both the eigenvectors and the corresponding eigenvalues form complex conjugate pairs. The arguments of the unitary eigenvalues play the role of round-trip Gouy phases χ_1 and χ_2 and determine the frequency spectrum according to equation (2.69). The spatial structure of the cavity modes is fully determined by the eigenvectors. They depend on the transverse reference plane that is taken as the start of a round trip. The eigenvalues are independent of the choice of the reference plane. As indicated in equation (2.61) and (2.62), the eigenvectors determine two 2×2 matrices $\mathsf{R}(z)$ and $\mathsf{T}(z)$, which vary along the optical axis of the lens guide that corresponds to the cavity. The Gaussian fundamental mode depends on these two matrices according to equation (2.64). Higher order modes arise after repeated application of bosonic raising operators as in equation (2.66), where these operators are specified by equations (2.59) and (2.60). These algebraic expressions can be used directly to calculate the mode profiles.

The spatial structure and physical properties of twisted cavity modes are significantly different from those of non-twisted (separable) cavity modes. The intensity and phase patterns of twisted modes tumble under propagation from one mirror to the other. As a result, there is orbital angular momentum in these modes. Moreover, the higher-order modes contain optical vortices in the transverse planes between the mirrors.

Since the paraxial wave equation (2.32), which describes free propagation of a paraxial beam, is identical in form to the Schrödinger equation of a free particle in two dimensions, the methods and results of this chapter can be applied to study the time evolution of the quantum states of a particle in free space. In the Schrödinger equation, the longitudinal coordinate z is replaced by time, while the two transverse coordinates x and y are replaced by three spatial coordinates. In that case, the approach discussed in this chapter involves three pairs of bosonic ladder operators, which characterize a complete and orthonormal set of exact wave-packet solutions of the Schrödinger equation.